FORCE-MOMENT CAPABILITIES OF PLANAR-PARALLEL MANIPULATORS USING DIFFERENT REDUNDANT-ACTUATION CONFIGURATIONS

Scott B. Nokleby
Faculty of Engineering and Applied Science
University of Ontario Institute of Technology
Oshawa, ON L1H 7K4, CANADA

ABSTRACT

This work investigates the force-moment capabilities of different redundant-actuation configurations for planar-parallel manipulators. A previously developed methodology for determining the force-moment capabilities of redundantly-actuated parallel manipulators using optimization and scaling factors is employed. The results show that different, symmetric redundant-actuation schemes yield substantial variations in the force-moment capabilities for the three branch, three-revolute joints per branch (3-RRR) manipulator. Configurations where all base and wrist joints are actuated or all elbow and wrist joints are actuated yielded better force-moment capabilities when compared to the actuation configuration where all base and elbow joints are actuated. The biggest difference in terms of force-moment capabilities was the maximum moment that could be sustained. The actuation configuration where all base and elbow joints actuated yielded the lowest maximum moment that could be sustained.

1. INTRODUCTION

This paper investigates the force-moment capabilities of different, symmetric, redundant-actuation configurations for planar-parallel manipulators. The force-moment capability of a manipulator is defined as the maximum wrench that can be applied (or sustained) by a manipulator for a given pose based on the limits of its actuators.

Redundant actuation in parallel manipulators can be divided into three categories. The first category features actuating some of the passive joints within the branches of a parallel manipulator. For example, consider the three-branch planar parallel manipulator with three-revolute joints per branch, the 3-RRR device [1]. For a non-redundant device, one joint per branch must be actuated. By actuating an additional joint in one or more branches, the manipulator is redundantly actuated. The second category of redundant manipulators are those that feature additional branches beyond the minimum necessary to actuate the device. Again considering the 3-RRR device, if an additional branch (featuring an actuated joint within the branch) is added to the device, the device would be redundantly actuated. The third category of redundantly-actuated parallel manipulators are devices that are a hybrid of the first two categories. This paper focuses on the first category, but the presented methodology could easily be applied to manipulators of the second and third category.

With redundant actuation, the solution to the inverse force problem (given the desired wrench to be applied by the platform, what are the required joint torques/forces) no longer has a unique solution. An infinity of possible solutions exists to the inverse force problem. This infinity of possible solutions allows the joint torques/forces to be optimized. The ability to optimize the

joint torques/forces and the elimination of force-unconstrained configurations[1] through redundant actuation has led to a growing interest in redundantly-actuated parallel manipulators (see for example [2–17]).

The goal of this paper is to investigate the force-moment capabilities of various redundant-actuation configurations for planar-parallel manipulators. To determine the force-moment capabilities, a methodology developed by Nokleby et al. [17] of determining the force-moment capabilities of redundantly-actuated parallel manipulators using scaling factors and optimization is employed.

To test the effects of different redundant-actuation configurations, the 3-RRR manipulator is used. Typically, the redundant-actuation configuration used for the 3-RRR manipulator is one where the base and elbow joints of each branch are actuated. For simplicity, this actuation configuration will be denoted 3-$\underline{\text{RR}}$R, where the underline indicates that the first and second joints of each branch are actuated. However, is this the best actuation scheme in terms of force-moment capabilities? Perhaps, the 3-$\underline{\text{R}}$R$\underline{\text{R}}$ or the 3-R$\underline{\text{RR}}$ actuation configurations may lead to better force-moment capabilities. The goal of this paper is to answer the above question.

The paper first briefly summarizes the methodology of Nokleby et al. [17]. Next, the force-moment capabilities for the 3-$\underline{\text{RR}}$R, the 3-$\underline{\text{R}}$R$\underline{\text{R}}$, and the 3-R$\underline{\text{RR}}$ actuation configurations are presented. This is followed by a discussion of the results. The paper finishes with proposals for future work and conclusions.

2. OPTIMIZATION-BASED METHODOLOGY FOR DETERMINING FORCE-MOMENT CAPABILITIES USING SCALING FACTORS [17]

In the forward force (FF) problem for manipulators, the actuated joint torques or forces are known and the output wrench is to be found. The output wrench modeled by the screw $\mathbf{F}_{app} = \left\{\mathbf{f}^{\mathrm{T}};\ \mathbf{m}^{\mathrm{T}}\right\}^{\mathrm{T}}$ can be calculated from:

$$\mathbf{F}_{app} = [\$'][\mathbf{D}]\tau \tag{1}$$

where τ is a vector of the actuated joint torques or forces and $[\$']$ is the matrix of associated reciprocal screw quantities[2]. In equation (1), $[\mathbf{D}]$ is a diagonal matrix which converts the vector of joint torques/forces to a vector of wrench intensities.

The inverse force (IF) problem solves for the actuated torques and forces required to sustain (or apply) a known wrench, $\mathbf{F}_{app}$, for a given location and orientation of the end effector. To determine the force-moment capabilities, however, one wants to find the maximum possible magnitude of $\mathbf{F}_{app}$ for a desired wrench direction. The unit wrench $\$_{\mathbf{F}}$ will be used to represent the desired wrench direction, therefore:

$$\mathbf{F}_{app} = f_{app}\$_{\mathbf{F}} \tag{2}$$

with f_{app} being the wrench intensity of $\mathbf{F}_{app}$. To generate a force-moment capability plot using the IF solution, one needs to find the maximum wrench intensity, f_{app}, in order to maximize the magnitude of $\mathbf{F}_{app}$, while still remaining within the torque/force limits of the actuated joints.

The first step is to find the vector of torques/forces, $\tau_{\$_{\mathbf{F}}}$, used to create the unit wrench $\$_{\mathbf{F}}$ in the direction of the desired $\mathbf{F}_{app}$, such that:

$$\$_{\mathbf{F}} = [\$'][\mathbf{D}]\tau_{\$_{\mathbf{F}}} \tag{3}$$

[1] A force-unconstrained configuration is a configuration in which the platform of a parallel manipulator cannot sustain or apply an arbitrary force and instantaneously gains an uncontrollable degree-of-freedom (DOF) of motion.

[2] Screw coordinates, associated reciprocal screw quantities, and the force problem in terms of screw algebra are described in Appendix A.

Referring to equation (3), the matrix formed by $[\$'][\mathbf{D}]$ is not square for the redundant case and an infinity of solutions exists to the IF problem. An optimization-based solution is necessary to find the best $\tau_{\$_\mathbf{F}}$ to use.

For redundantly-actuated manipulators, the solution to the IF problem can be broken into a particular solution and a homogeneous solution:

$$\tau_{\$_\mathbf{F}} = \tau_{\$_{\mathbf{F}\text{particular}}} + \tau_{\$_{\mathbf{F}\text{homogeneous}}} \tag{4}$$

The particular solution, $\tau_{\$_{\mathbf{F}\text{particular}}}$, satisfies:

$$[\$'][\mathbf{D}]\tau_{\$_{\mathbf{F}\text{particular}}} = \$_\mathbf{F} \tag{5}$$

The homogeneous solution, $\tau_{\$_{\mathbf{F}\text{homogeneous}}}$, satisfies:

$$[\$'][\mathbf{D}]\tau_{\$_{\mathbf{F}\text{homogeneous}}} = 0 \tag{6}$$

which is the null-space solution.

For any solution of $\tau_{\$_{\mathbf{F}\text{particular}}}$, $\tau_{\$_{\mathbf{F}\text{homogeneous}}}$ can be solved for using Singular Value Decomposition (SVD). Performing SVD on the matrix $[\$'][\mathbf{D}]$ of size $m \times n$ and rank r yields the matrices $\mathbf{S}_{m\times n}$, $\mathbf{U}_{m\times m}$, and $\mathbf{V}_{n\times n}$. The matrix $\mathbf{S}$ is a diagonal matrix of the square roots of the non-zero eigenvalues of $\left([\$'][\mathbf{D}]\right)\left([\$'][\mathbf{D}]\right)^{\mathrm{T}}$ and $\left([\$'][\mathbf{D}]\right)^{\mathrm{T}}\left([\$'][\mathbf{D}]\right)$. The matrices $\mathbf{U}$ and $\mathbf{V}$ are both orthogonal matrices and provide bases for the four fundamental subspaces of $[\$'][\mathbf{D}]$ [18]. The last $n-r$ columns of $\mathbf{V}$ span the null space of $[\$'][\mathbf{D}]$ and are denoted $\mathbf{V}'$. Therefore, the homogeneous solution can be expressed as:

$$\tau_{\$_{\mathbf{F}\text{homogeneous}}} = \mathbf{V}'\upsilon \tag{7}$$

where υ is any $(n-r)\times 1$ vector which is mapped by $\mathbf{V}'$ into the null-space torque/force for the given $[\$'][\mathbf{D}]$. Physically, the resultant $\tau_{\$_{\mathbf{F}\text{homogeneous}}}$ is a set of actuator outputs which result in no output wrench being applied by the manipulator. The torques/forces are such that they apply what is referred to as an internal force.

Using the Moore-Penrose pseudo-inverse solution to find $\tau_{\$_{\mathbf{F}\text{particular}}}$, as it satisfies equation (5), and equation (7) to find $\tau_{\$_{\mathbf{F}\text{homogeneous}}}$ yields:

$$\tau_{\$_\mathbf{F}} = \left([\$'][\mathbf{D}]\right)^{+}\$_\mathbf{F} + \mathbf{V}'\upsilon \tag{8}$$

To achieve the largest force capabilities requires finding the υ that minimizes the maximum absolute value of the normalized torque vector, where the normalized torque vector $\widehat{\tau}_{\$_\mathbf{F}}$ is defined as:

$$\widehat{\tau}_{\$_\mathbf{F}} = \left\{ \cdots \quad \frac{\tau_{\$_\mathbf{F}j_i}}{\tau_{j_i\max}} \quad \cdots \right\} \tag{9}$$

This problem can be expressed as the optimization problem:

$$\text{minimize } f(\upsilon) = \max\left(\left|\widehat{\tau}_{\$_\mathbf{F}}\right|\right) \tag{10}$$

In order to ensure a continuous objective function, the objective function of equation (10) can be approximated by taking a high p-norm of $\widehat{\tau}_{\$_\mathbf{F}}$. Therefore, the optimization problem becomes:

$$\text{minimize } f(\upsilon) = \left\|\widehat{\tau}_{\$_\mathbf{F}}\right\|_p \tag{11}$$

For this work, the value of the p-norm was set to 100 and the optimization problem was solved using the MATLAB® Optimization Toolbox routine `fminunc`. The routine `fminunc` uses the Broyden-Fletcher-Goldfarb-Shanno (BFGS) quasi-Newton algorithm with a mixed quadratic and cubic line search to solve the unconstrained optimization problem [19].

Solving the optimization problem of equation (11) and substituting the solution into equation (8) will yield an optimal $\tau_{\$_\mathbf{F}}$.

Since all maximum actuated joint torque and force limits, $\tau_{j_i\,\max}$, are known for all actuated joints j of each branch i of the manipulator, scaling factors for each actuated joint can be found using:

$$sf_{j_i} = \left| \frac{\tau_{j_i\,\max}}{\tau_{\$_\mathbf{F} j_i}} \right| \tag{12}$$

where sf_{j_i} is the scaling factor and $\tau_{\$_\mathbf{F} j_i}$ is the torque/force of the j^{th} actuated joint of the i^{th} branch for a unit wrench $\$_\mathbf{F}$ in the desired force direction. The scaling factors of equation (12) can be placed in a set. The scaling factor (SF) in this set with the minimum value is the maximum factor which all joint torques/forces can be scaled by and still remain at or below their corresponding maximum values, i.e.:

$$SF = \min_{j_i}(sf_{j_i}) \tag{13}$$

The maximum wrench, $\mathbf{F}_{app}$, that can be applied in the direction $\$_\mathbf{F}$ is:

$$\mathbf{F}_{app} = SF[\$'][\mathbf{D}]\tau_{\$_\mathbf{F}} \tag{14}$$

Since $[\$'][\mathbf{D}]\tau_{\$_\mathbf{F}}$ generates the unit wrench $\$_\mathbf{F}$, the maximum possible wrench intensity f_{app} of the screw quantity $\mathbf{F}_{app}$ is:

$$f_{app} = SF \tag{15}$$

To create a force-moment capability plot using the IF solution, $\$_\mathbf{F}$ is varied through all possible directions.

3. FORCE-MOMENT CAPABILITIES

The manipulator being considered is the three-branch, three-revolute joints per branch (3-RRR), planar parallel manipulator. Figure 1 shows the layout of the 3-RRR manipulator. The manipulator's dimensions and actuation capabilities are modeled after the Reconfigurable Planar Parallel Manipulator (RPPM) [20]. For the RPPM, the link lengths and platform edge lengths are all equal to 0.200 m, i.e., ρ_1 to $\rho_6 = l_2 = l_3 = 0.200$ m and $\alpha = 60°$. The bases of the branches are all 0.500 m apart from each other. The maximum torque capability for each actuated joint of the RPPM is ± 4.2 Nm.

The reference frame was selected to be coincident with frame 3 of branch 1 (see Figure 1). The complete kinematic model used for the RPPM can be found in [17].

The unit wrench $\$_\mathbf{F}$ in the platform frame used to generate the force-moment capability plots was defined as:

$$^{plat}\$_\mathbf{F} = \{\cos(\beta),\ \sin(\beta),\ 0;\ 0,\ 0,\ m_z\}^{\mathrm{T}}$$

where β was varied between 0 and 2π in increments of $\pi/360$ and m_z was varied between -15 Nm and 15 Nm in a varied step size (see Table 1).

For the force-moment capability plots, three different actuation configurations were considered: 3-$\underline{\text{RR}}$R; 3-R$\underline{\text{RR}}$; and 3-R$\underline{\text{R}}$R. For each actuation configuration, three orientations of the platform were tested while the platform's position was fixed at the centre of the manipulator's workspace ($x_0 = 0.250$ m and $y_0 = 0.144$ m). The platform orientations (ϕ's) used were $-45°$, 0, and $45°$.

Figures 2, 3, and 4 present the force-moment capabilities for the three actuation configurations and each of the three platform orientations. Figure 2 shows the force-moment capabilities when

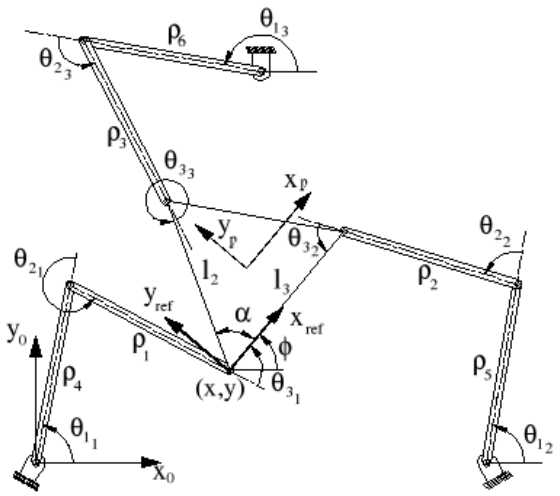

Figure 1: The layout of the 3-RRR manipulator.

Table 1: Step sizes used for m_z.

m_z Range (Nm)	m_z Step Size (Nm)
-100.00 to -15.00	5.00
-15.00 to -1.00	0.50
-1.00 to -0.10	0.05
-0.10 to 0.00	0.005
0.00 to 0.10	0.005
0.10 to 1.00	0.05
1.00 to 15.00	0.50
15.00 to 100.00	5.00

$\phi = -45°$, Figure 3 shows the force-moment capabilities when $\phi = 0$, and Figure 4 shows the force-moment capabilities when $\phi = 45°$. It is important to note that for Figures 2, 3, and 4 that the scales used for the moments are not the same for the three different actuation configurations.

Table 2 shows the maximum force mangitude and the maximum moment that can be sustained by each of the actuation configurations for each of the platform orientations.

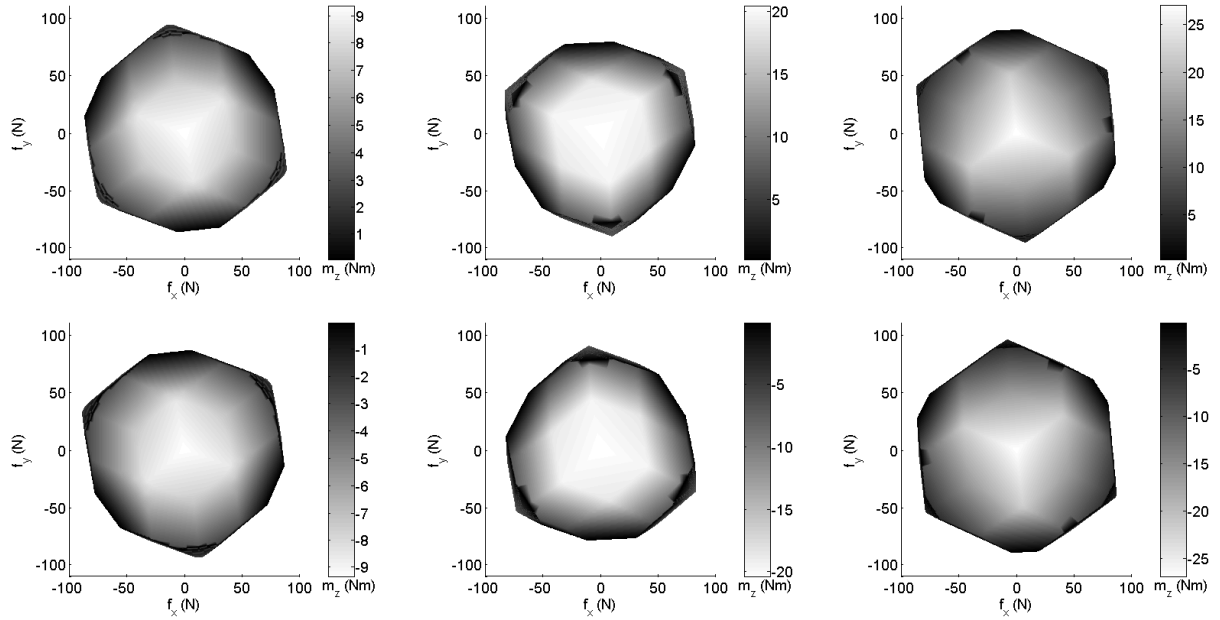

Figure 2: Force-moment capabilities when $\phi = -45°$: a) 3-$\underline{\text{RR}}$R configuration, b) 3-$\underline{\text{R}}$R$\underline{\text{R}}$ configuration, c) 3-R$\underline{\text{RR}}$ configuration. Note that the first row of plots corresponds to $+m_z$ and the second row of plots corresponds to $-m_z$.

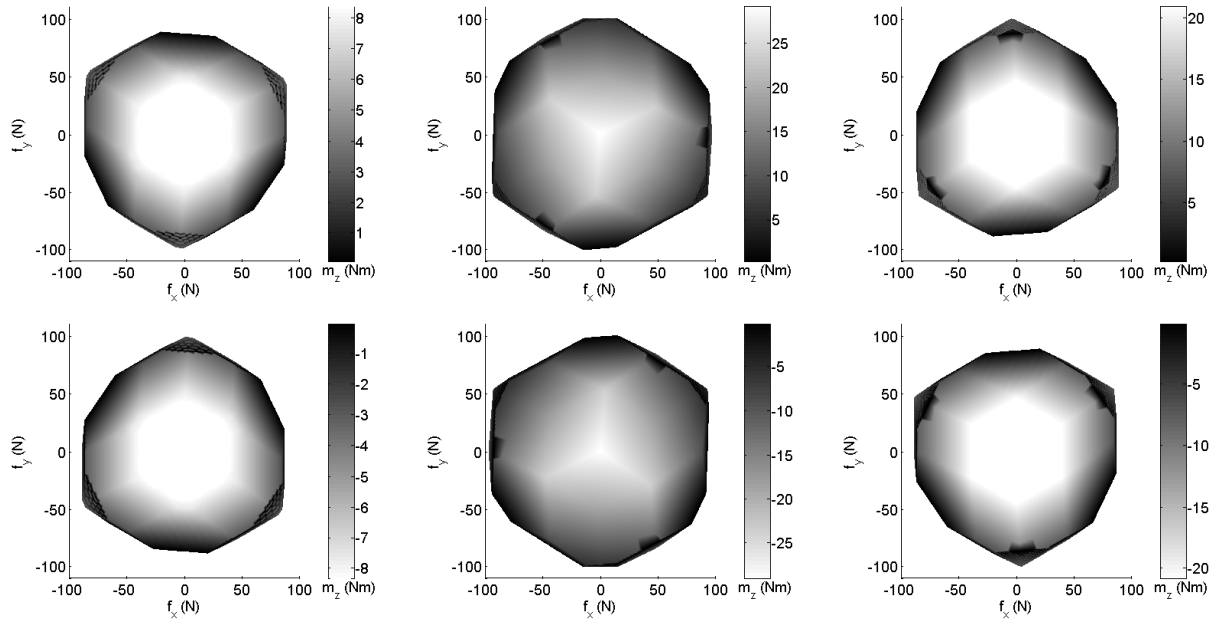

Figure 3: Force-moment capabilities when $\phi = 0$: a) 3-$\underline{\text{RR}}$R configuration, b) 3-$\underline{\text{R}}$R$\underline{\text{R}}$ configuration, c) 3-R$\underline{\text{RR}}$ configuration. Note that the first row of plots corresponds to $+m_z$ and the second row of plots corresponds to $-m_z$.

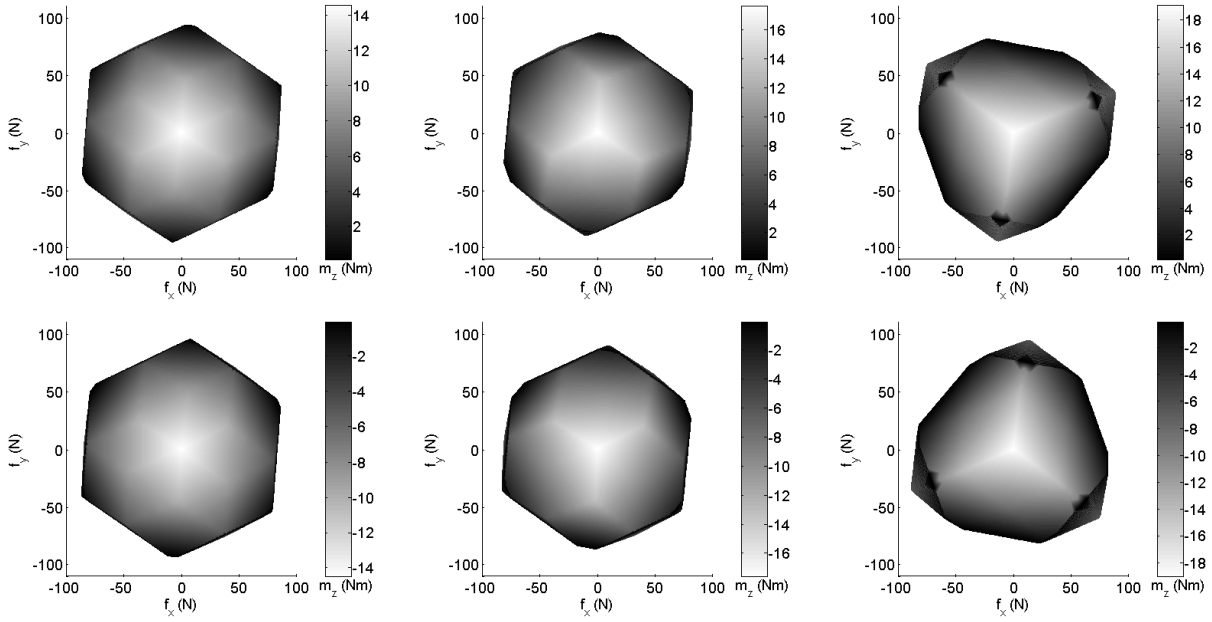

Figure 4: Force-moment capabilities when $\phi = 45°$: a) 3-$\underline{\text{RR}}$R configuration, b) 3-R$\underline{\text{RR}}$ configuration, c) 3-R$\underline{\text{RR}}$ configuration. Note that the first row of plots corresponds to $+m_z$ and the second row of plots corresponds to $-m_z$.

Table 2: Maximum force magnitude and maximum moment.

Configuration	ϕ (°)	Maximum Force Magnitude (N)	Maximum Moment (Nm)
3-$\underline{\text{RR}}$R	-45	94.17	$\pm$9.41
3-R$\underline{\text{RR}}$	-45	90.31	$\pm$20.59
3-R$\underline{\text{RR}}$	-45	95.31	$\pm$27.14
3-$\underline{\text{RR}}$R	0	98.51	$\pm$8.40
3-R$\underline{\text{RR}}$	0	106.74	$\pm$29.28
3-R$\underline{\text{RR}}$	0	99.93	$\pm$21.00
3-$\underline{\text{RR}}$R	45	95.53	$\pm$14.62
3-R$\underline{\text{RR}}$	45	89.87	$\pm$17.75
3-R$\underline{\text{RR}}$	45	95.11	$\pm$19.17

4. DISCUSSION

Referring to Table 2 and Figures 2, 3, and 4, it is clear that the force-moment capabilities differ for the three different actuation configurations. In terms of the maximum magnitude of force that can be sustained for the three configurations, there is not as much variance between the 3-RRR, 3-RRR, and 3-RRR configurations. For the three poses, the maximum magnitude of force varied from 5% to 8%.

The real difference in the capabilities of the three actuation configurations is in terms of the maximum moments that can be sustained. Both the 3-RRR and 3-RRR configurations yielded better moment capabilities than the 3-RRR configuration. For the $\phi = -45°$ and the $\phi = 0$ poses, the maximum moment that could be sustained for the 3-RRR and 3-RRR configurations was over twice what could be sustained by the 3-RRR configuration.

The question posed at the start of the paper was: Is the 3-RRR configuration the best actuation scheme in terms of force-moment capabilities? Although the results are not exhaustive, having only considered three different manipulator poses, the preliminary results indicate that the 3-RRR configuration may not be the best actuation scheme in terms of force-moment capabilities. The results show that actuation configurations where the platform joints of each branch were actuated (3-RRR and 3-RRR) yielded better moment capabilities when compared to the actuation configuration without the platform joints actuated (3-RRR). The differences in force-moment capabilities is most likely due to variations in the internal wrenches generated by the various redundant actuation schemes.

One could raise the point that the 3-RRR actuation configuration would minimize the inertia of the platform when compared to the 3-RRR and 3-RRR actuation configurations. This would be true if the motors were mounted directly at the joints. However, if one were to base-mount all motors and use chain or belt drives to actuate the non-base joints, this argument can easily be dismissed.

5. FUTURE WORK

As pointed out, the results presented here are not exhaustive since only three poses were considered. One avenue of future work would be a more exhaustive analysis of the force-moment capabilties over a wider range of the manipulator's workspace.

This work only foucssed on symmetric actuation configurations. Another possible topic for future exploration would be to investigate the effects of non-symmetric, redundant-actuation schemes.

A final topic of future research would be to investigate the force-moment capabilties of planar-parallel manipulators incorporating additional redundant branches.

6. CONCLUSIONS

The force-moment capabilites of a redundantly-actuated, planar-parallel manipulator using three different actuation configurations were investigated. It was shown that both the 3-RRR and 3-RRR actuation configurations yielded better force-moment capabilities when compared to the 3-RRR actuation configuration. The biggest difference in terms of force-moment capabilty was the maximum moment that could be sustained, with the 3-RRR and 3-RRR actuation configurations being able to sustain over twice the maximum moment of the 3-RRR actuation configuration for certain poses.

ACKNOWLEDGEMENTS

The author wishes to thank Flavio Firmani of the University of Victoria for creating Figure 1. The author also thanks his former colleagues at the Robotics and Mechanisms Laboratory, University of Victoria, who co-authored the work on the optimization-based methodology for determining force-moment capabilities of parallel manipulators using scaling factors [17] that formed the basis for generating the results presented in this paper. The anonymous reviewers are also thanked for their comments to improve the paper.

REFERENCES

[1] C. Gosselin and J. Angeles, "The Optimum Kinematic Design of a Planar Three-Degree-of-Freedom Parallel Manipulator," *Transactions of the ASME, Journal of Mechanisms, Transmissions, and Automation in Design*, vol. 110, no. 1, pp. 35–41, 1988.

[2] R. Kurtz and V. Hayward, "Multiple-Goal Kinematic Optimization of a Parallel Spherical Mechanism with Actuator Redundancy," *IEEE Transactions on Robotics and Automation*, vol. 8, no. 5, pp. 644–651, 1992.

[3] D. R. Kerr, M. Griffis, D. J. Sanger, and J. Duffy, "Redundant Grasps, Redundant Manipulators, and Their Dual Relationship," *Journal of Robotic Systems*, vol. 9, no. 7, pp. 973–1000, 1992.

[4] S. Lee and S. Kim, "Kinematic Feature Analysis of Parallel Manipulator Systems," in *Proceedings of the 1994 IEEE International Conference on Robotics and Automation*, (May 8-13, San Diego, California, USA), pp. 77–82, 1994.

[5] P. Buttolo and B. Hannaford, "Advantages of Actuation Redundancy for the Design of Haptic Displays," in *Proceedings of the 1995 ASME International Mechanical Engineering Congress and Exposition - Part 2*, (November 12-17, San Francisco, California, USA), pp. 623–630, 1995.

[6] J.-P. Merlet, "Redundant Parallel Manipulators," *Laboratory Robotics and Automation*, vol. 8, no. 1, pp. 17–24, 1996.

[7] L. Beiner, "Redundant Actuation of a Closed-Chain Device," *Advanced Robotics*, vol. 11, no. 3, pp. 233–245, 1997.

[8] B. Dasgupta and T. S. Mruthyunjaya, "Force Redundancy in Parallel Manipulators: Theoretical and Practical Issues," *Mechanism and Machine Theory*, vol. 33, no. 6, pp. 727–742, 1998.

[9] H. S. Kim and Y. J. Choi, "The Kinetostatic Capability Analysis of Robotic Manipulators," in *Proceedings of the 1999 IEEE/RSJ International Conference on Intelligent Robots and Systems*, (October 17-21, Kyongju, South Korea), pp. 1241–1246, 1999.

[10] L. J. Gonzalez and S. V. Sreenivasan, "Representational Singularities in the Torque Optimization Problem of an Active Closed Loop Mechanism," *Mechanism and Machine Theory*, vol. 35, no. 6, pp. 871–886, 2000.

[11] S. H. Lee, B.-J. Yi, S. H. Kim, and Y. K. Kwak, "Control of Impact Disturbance by Redundantly Actuated Mechanism," in *Proceedings of the 2001 IEEE International Conference on Robotics and Automation*, (May 21-26, Seoul, South Korea), pp. 3734–3741, 2001.

[12] G. F. Liu, Y. L. Wu, X. Z. Wu, Y. Y. Kuen, and Z. X. Li, "Analysis and Control of Redundant Parallel Manipulators," in *Proceedings of the 2001 IEEE International Conference on Robotics and Automation*, (May 21-26, Seoul, Korea), pp. 3748–3754, 2001.

[13] L. L. Ganovski, P. Fisette, and J.-C. Samin, "Modeling of Overactuated Closed-Loop Mechanisms with Singularities: Simulation and Control," in *Proceedings of the 2001 ASME Design Engineering Technical Conferences and the Computers and Information in Engineering Conference*, (September 9-12, Pittsburgh, Pennsylvania, USA), 8 pages, 2001.

[14] H. Cheng, G. F. Liu, Y. K. Yiu, Z. H. Xiong, and Z. X. Li, "Advantages and Dynamics of Parallel Manipulators with Redundant Actuation," in *Proceedings of the 2001 IEEE/RSJ International Conference on Intelligent Robots and Systems*, (October 29 - November 3, Maui, Hawaii, USA), pp. 171–176, 2001.

[15] H. Cheng, Y.-K. Yiu, and Z. Li., "Dynamics and Control of Redundantly Actuated Parallel Manipulators," *IEEE Transactions on Mechatronics*, vol. 8, no. 4, pp. 483–491, 2003.

[16] F. Firmani and R. P. Podhorodeski, "Force-Unconstrained Poses for a Redundantly-Actuated Planar Parallel Manipulator," *Mechanism and Machine Theory*, vol. 39, no. 5, pp. 459–476, 2004.

[17] S. B. Nokleby, R. Fisher, R. P. Podhorodeski, and F. Firmani, "Force Capabilities of Redundantly-Actuated Parallel Manipulators," *Mechanism and Machine Theory*, vol. 40, no. 5, pp. 578–599, 2005.

[18] G. Strang, *Linear Algebra and Its Applications - Third Edition*. San Diego, California, USA: Harcourt Brace Jovanovich, 1988.

[19] MathWorks, *Optimization Toolbox User's Guide - Version 2*. Natick, Massachusetts, USA: The MathWorks, Inc., 2001.

[20] R. Fisher, R. P. Podhorodeski, and S. B. Nokleby, "Design of a Reconfigurable Planar Parallel Manipulator," *Mechanism and Machine Theory*, vol. 21, no. 12, pp. 665–675, 2004.

[21] R. S. Ball, *A Treatise on the Theory of Screws*. Cambridge, United Kingdom: Cambridge University Press, 1900 (Reprinted 1998).

[22] K. H. Hunt, *Kinematic Geometry of Mechanisms*. Toronto, Ontario, Canada: Oxford University Press, 1978 (Reprinted 1990).

[23] O. Bottema and B. Roth, *Theoretical Kinematics*. New York, New York, USA: Dover Publications, Inc., 1979 (Reprinted 1990).

[24] K. H. Hunt, "Robot Kinematics - A Compact Analytic Inverse Solution for Velocities," *Transactions of the ASME, Journal of Mechanisms, Transmissions, and Automation in Design*, vol. 109, no. 1, pp. 42–49, 1987.

APPENDIX A: PARALLEL MANIPULATOR KINEMATICS USING SCREW ALGEBRA [3]

This appendix presents an overview of the use of screw algebra in parallel manipulator kinematics. The reader is referred to the works of Ball [21], Hunt [22], and Bottema and Roth [23] for more detailed information on screw theory.

Screws

Screw Coordinates, Plücker Coordinates, and Pitch

A screw ($\mathbf{S}$) is a line in space having an associated linear pitch. Screws can be represented as:

$$\mathbf{S} = \left\{ \begin{array}{c} \mathbf{s} \\ \mathbf{s}_o \end{array} \right\} = \lambda \left\{ \begin{array}{c} \boldsymbol{l} \\ \boldsymbol{l}_o + p\boldsymbol{l} \end{array} \right\} \tag{16}$$

where $\mathbf{s}$ and $\mathbf{s}_o$ are the screw coordinates, $\boldsymbol{l}$ and $\boldsymbol{l}_o$ are the Plücker coordinates of the line, λ is an associated magnitude, and p is the pitch of the screw [22, 24]. The pitch of a screw can be found from:

$$p = \frac{\mathbf{s} \cdot \mathbf{s}_o}{\|\mathbf{s}\|}$$

A screw is said to be a unit or normalized screw ($) if $\|\mathbf{s}\| = 1$ or in the case where $\mathbf{s} = \mathbf{0}_{3\text{x}1}$, if $\|\mathbf{s}_o\| = 1$ [24].

For manipulators, a revolute joint can be represented by a zero-pitch unit screw $\$_{rev} = \{ \quad \boldsymbol{l}^{\mathrm{T}}; \quad \boldsymbol{l}_o^{\mathrm{T}} \}^{\mathrm{T}}$ and a prismatic joint can be represented by an infinite-pitch unit screw which when normalized to the ∞-pitch gives $\$_{pris} = \{\mathbf{0}_{3\text{x}1}^{\mathrm{T}}; \quad \boldsymbol{l}^{\mathrm{T}}\}^{\mathrm{T}}$.

The screw coordinates of the joints of a manipulator can be found from:

$${}^{ref}\$_{j_i} = \left\{ \begin{array}{c} {}^{ref}\widehat{\mathbf{z}}_{j_i} \\ {}^{ref}\widehat{\mathbf{z}}_{j_i} \times {}^{ref}\mathbf{r}_{j_i \to p_{ee}} \end{array} \right\}_{revolute} \text{ or } = \left\{ \begin{array}{c} \mathbf{0}_{3\text{x}1} \\ {}^{ref}\widehat{\mathbf{z}}_{j_i} \end{array} \right\}_{prismatic} \tag{17}$$

where $\widehat{\mathbf{z}}_{j_i}$ denotes the unit vector of the j^{th} joint axis direction of the i^{th} branch, p_{ee} denotes a point coincident with the origin of F_{ref} and attached to the end-effector, and $\mathbf{r}_{j_i \to p_{ee}}$ denotes a vector from a point on the axis of joint j_i to the point p_{ee}. Note that for zero-pitch and infinite-pitch unit screws, the screw coordinates are equivalent to the Plücker coordinates.

Screw Transformations

A screw transformation is defined as:

$${}^{ref_a}_{ref_b}\mathbf{T}_{\mathbf{S}} = \left[\begin{array}{cc} {}^{ref_a}_{ref_b}\mathbf{R} & \mathbf{0}_{3\text{x}3} \\ {}^{ref_a}\widetilde{\mathbf{p}}_{o_a \to o_b} \, {}^{ref_a}_{ref_b}\mathbf{R} & {}^{ref_a}_{ref_b}\mathbf{R} \end{array} \right] \tag{18}$$

where ${}^{ref_a}_{ref_b}\mathbf{R}$ is a 3x3 rotation matrix and ${}^{ref_a}\widetilde{\mathbf{p}}_{o_a \to o_b}$ is a 3x3 cross product skew-symmetric matrix based on the components of a vector, ${}^{ref_a}\mathbf{p}_{o_a \to o_b} = {}^{ref_a}\{p_{x_{o_a \to o_b}}, p_{y_{o_a \to o_b}}, p_{z_{o_a \to o_b}}\}^{\mathrm{T}}$, from the origin of F_{ref_a} to the origin of F_{ref_b}. The cross product skew-symmetric matrix ${}^{ref_a}\widetilde{\mathbf{p}}_{o_a \to o_b}$ is:

$${}^{ref_a}\widetilde{\mathbf{p}}_{o_a \to o_b} = \left[\begin{array}{ccc} 0 & -p_{z_{o_a \to o_b}} & p_{y_{o_a \to o_b}} \\ p_{z_{o_a \to o_b}} & 0 & -p_{x_{o_a \to o_b}} \\ -p_{y_{o_a \to o_b}} & p_{x_{o_a \to o_b}} & 0 \end{array} \right] \tag{19}$$

[3] This appendix originally appeared in [17].

Reciprocal Screws

Let the screw quantity $\mathbf{A} = \{\mathbf{a}^{\mathrm{T}};\ \mathbf{a}_o^{\mathrm{T}}\}^{\mathrm{T}}$ represent the velocity of a body and the screw quantity $\mathbf{B} = \{\mathbf{b}^{\mathrm{T}};\ \mathbf{b}_o^{\mathrm{T}}\}^{\mathrm{T}}$ represent a wrench acting on the body. If the power developed by wrench $\mathbf{B}$ acting on the body moving with velocity $\mathbf{A}$ is zero, the screw quantities $\mathbf{A}$ and $\mathbf{B}$ are said to be reciprocal to one another [22]. Mathematically, the two screws, $\mathbf{A}$ and $\mathbf{B}$, are reciprocal if their reciprocal product is zero:

$$\mathbf{A} \circledast \mathbf{B} = \mathbf{a} \cdot \mathbf{b}_o + \mathbf{a}_o \cdot \mathbf{b} = 0 \tag{20}$$

where $\circledast$ denotes a reciprocal product between two screws.

Parallel Manipulator Kinematics Using Screws

Velocity Solutions

The end-effector or platform twist ($\mathbf{V}$) of a manipulator is defined as:

$$\mathbf{V} = \left\{ \begin{array}{c} \omega \\ \mathbf{v} \end{array} \right\} \tag{21}$$

where ω is the angular velocity and $\mathbf{v}$ is the translational velocity.

Assume a parallel manipulator has m branches. For the i^{th} branch, it is assumed that there are l_i joints of which n_i joints are actuated. For the actuated joint j of the i^{th} branch, a unit screw, $\$'_{j_i}$, reciprocal to all joints of branch i except for the actuated joint j can be found, i.e.:

$$\$_{k_i} \circledast \$'_{j_i} = 0, \text{ for } k = 1 \text{ to } l_i,\ j \neq k \tag{22}$$

Note that for the i^{th} branch of the manipulator:

$$\mathbf{V} \circledast \$'_{j_i} = \sum_{k=1}^{l_i} \dot{q}_{k_i} \$_{k_i} \circledast \$'_{j_i} = \dot{q}_{j_i} \$_{j_i} \circledast \$'_{j_i}, \text{ for } j = 1 \text{ to } n_i \tag{23}$$

where $\dot{q}$ denotes a joint rate. The joint rate of the actuated joint j of the i^{th} branch can be found as:

$$\dot{q}_{j_i} = \frac{\mathbf{V} \circledast \$'_{j_i}}{\$_{j_i} \circledast \$'_{j_i}} \tag{24}$$

Define the reciprocal screw matrix $[\$']$ as:

$$[\$'] = \left[\begin{array}{ccc} \cdots & \$'_{j_i} & \cdots \end{array} \right] \tag{25}$$

where $i = 1$ to m and $j = 1$ to n_i and define the diagonal matrix $\mathbf{D}$ of the inverses of the reciprocal products of the actuated joints and their associated reciprocal screws as:

$$\mathbf{D} = \left[\begin{array}{ccc} \ddots & & \mathbf{0} \\ & \frac{1}{\$_{j_i} \circledast \$'_{j_i}} & \\ \mathbf{0} & & \ddots \end{array} \right] \tag{26}$$

The inverse velocity solution of a parallel manipulator can thus be expressed in matrix form as:

$$\dot{\mathbf{q}} = \mathbf{D} \left([\mathbf{\Delta}] \, [\$'] \right)^{\mathrm{T}} \mathbf{V} = \mathbf{D} [\$']^{\mathrm{T}} \, [\mathbf{\Delta}] \, \mathbf{V} \tag{27}$$

where the matrix $[\mathbf{\Delta}]$ is an interchange operator that transforms screws between axis-coordinate order to ray-coordinate order and is defined as:

$$[\mathbf{\Delta}] = \begin{bmatrix} \mathbf{0}_{3x3} & \mathbf{I}_{3x3} \\ \mathbf{I}_{3x3} & \mathbf{0}_{3x3} \end{bmatrix} \tag{28}$$

Solving for $\mathbf{V}$ in equation (27) allows the forward velocity solution of a non-redundantly-actuated parallel manipulator to be expressed in matrix form as:

$$\mathbf{V} = \begin{Bmatrix} \omega \\ \mathbf{v} \end{Bmatrix} = \left(\mathbf{D}[\$']^{\mathrm{T}}[\mathbf{\Delta}]\right)^{-1}\dot{\mathbf{q}} = [\mathbf{\Delta}]\,[\$']^{-\mathrm{T}}\mathbf{D}^{-1}\dot{\mathbf{q}} \tag{29}$$

where the fact that $[\mathbf{\Delta}]^{-1} = [\mathbf{\Delta}]$ has been utilized.

Force Solutions

The wrench ($\mathbf{F}$) applied by the end-effector or platform of a manipulator is defined as:

$$\mathbf{F} = \begin{Bmatrix} \mathbf{f} \\ \mathbf{m} \end{Bmatrix} \tag{30}$$

where $\mathbf{f}$ is the force applied and $\mathbf{m}$ is the moment applied. The wrench applied by a parallel manipulator is the sum of the wrenches applied by each actuated joint of the manipulator. Therefore, the forward static force solution for a parallel manipulator is given by:

$$\mathbf{F} = \begin{Bmatrix} \mathbf{f} \\ \mathbf{m} \end{Bmatrix} = \sum_{i=1}^{m}\left(\sum_{j=1}^{n_i}\$'_{j_i}\,w_{j_i}\right)$$

where w_{j_i} is the wrench intensity applied by the j^{th} joint of the i^{th} branch. In matrix form, the forward static force solution can be expressed as:

$$\mathbf{F} = \begin{Bmatrix} \mathbf{f} \\ \mathbf{m} \end{Bmatrix} = [\$']\mathbf{w} \tag{31}$$

where $\mathbf{w}$ is a vector of wrench intensities acting on the screws of $[\$']$.

The relationship between the wrench intensity w_{j_i} and the joint torque/force τ_{j_i} for joint j of the i^{th} branch is:

$$w_{j_i} = \frac{\tau_{j_i}}{\$_{j_i} \circledast \$'_{j_i}} \tag{32}$$

In matrix form, the relationship between the wrenches and the joint torques/forces for a parallel manipulator can be expressed as:

$$\mathbf{w} = \mathbf{D}\tau \tag{33}$$

Substituting equation (33) into equation (31) yields the forward static force solution relating the joint torques/forces to the force being applied by the manipulator:

$$\mathbf{F} = \begin{Bmatrix} \mathbf{f} \\ \mathbf{m} \end{Bmatrix} = [\$']\mathbf{D}\tau \tag{34}$$

The inverse static force solution for a non-redundantly-actuated parallel manipulator is:

$$\tau = \left([\$']\mathbf{D}\right)^{-1}\mathbf{F} = \mathbf{D}^{-1}[\$']^{-1}\mathbf{F} \tag{35}$$